

Article

Fabrication of Graphene Oxide-Decorated Mesoporous NiFe₂O₄ as an Electrocatalyst in the Hydrogen Gas Evolution Reaction

Afiten R. Sanjaya ¹, Salsabila Amanda ^{1,2}, Tribidasari A. Ivandini ¹, Faisal Abnisa ³, Grandprix T. M. Kadja ^{4,5,6}, Uji Pratomo ⁷, Yatimah Alias ⁸ and Munawar Khalil ^{1,2,*}

¹ Department of Chemistry, Faculty of Mathematics and Natural Sciences, Universitas Indonesia, Depok 16424, Indonesia

² Low Dimension Materials Laboratory, Department of Chemistry, Faculty of Mathematics and Natural Sciences, Universitas Indonesia, Depok 16424, Indonesia

³ Department of Chemical and Materials Engineering, Faculty of Engineering, King Abdulaziz University, Rabigh 21911, Saudi Arabia

⁴ Division of Inorganic and Physical Chemistry, Faculty of Mathematics and Natural Sciences, Institut Teknologi Bandung, Jalan Ganesha No. 10, Bandung 40132, Indonesia

⁵ Research Center for Nanosciences and Nanotechnology, Institut Teknologi Bandung, Jalan Ganesha No. 10, Bandung 40132, Indonesia

⁶ Center for Catalysis and Reaction Engineering, Institut Teknologi Bandung, Jalan Ganesha No. 10, Bandung 40132, Indonesia

⁷ Department of Chemistry, Faculty of Mathematics and Natural Sciences, Universitas Padjadjaran, Jl. Raya Bandung-Sumedang Km.21, Sumedang 45363, Indonesia

⁸ Department of Chemistry, Faculty of Science, University of Malaya, Kuala Lumpur 50603, Malaysia

* Correspondence: mkhalil@sci.ui.ac.id

Abstract: An electrocatalyst for the hydrogen evolution reaction has been successfully synthesized from graphene oxide (GO) decorated with the mesoporous NiFe₂O₄. A high catalytic activity performance was reached by using the GCE surface as a conductor, and the synthesized composite contained GO/NiFe₂O₄. Based on the results, the as-prepared electrocatalyst exhibited a high overpotential for the HER reaction of 36 mV vs. RHE at a 10 mA current density, with an electrochemical active surface area (ECSA) of 3.18×10^{-4} cm². Additionally, the electrocatalyst demonstrated a considerably good performance after the 9000 s stability test. It is believed that such an enhancement in electrocatalytic activity was due to the synergistic effect between the unique porosity feature of the mesoporous NiFe₂O₄, which may provide a more active surface, and the high conductivity of the GO.

Keywords: hydrogen evolution reaction; electrocatalyst; mesoporous NiFe₂O₄; graphene oxide; composite; renewable energy



Citation: Sanjaya, A.R.; Amanda, S.; Ivandini, T.A.; Abnisa, F.; Kadja, G.T.M.; Pratomo, U.; Alias, Y.; Khalil, M. Fabrication of Graphene Oxide-Decorated Mesoporous NiFe₂O₄ as an Electrocatalyst in the Hydrogen Gas Evolution Reaction. *Designs* **2023**, *7*, 26. <https://doi.org/10.3390/designs7010026>

Academic Editor: Surender Reddy Salkuti

Received: 8 December 2022

Revised: 20 January 2023

Accepted: 30 January 2023

Published: 1 February 2023



Copyright: © 2023 by the authors. Licensee MDPI, Basel, Switzerland. This article is an open access article distributed under the terms and conditions of the Creative Commons Attribution (CC BY) license (<https://creativecommons.org/licenses/by/4.0/>).

1. Introduction

Hydrogen gas is one of the most promising renewable fuels that could be used in the future, owing to its high energy density with no greenhouse gas emissions [1,2]. However, as an alternative energy resource, hydrogen needs further development—especially in the efficiency of the hydrogen production plants [3,4]. Currently, hydrogen production is still considered too time-consuming, with huge fossil fuel emissions [3–5]. Nowadays, most hydrogen production in the industry is dominated by the steam reforming of natural gas, the partial oxidation of hydrocarbons, or coal gasification. Therefore, a more environmentally friendly way of producing hydrogen is still desired. Recently, water electrolysis has received significant attention and is considered the most promising alternative and sustainable way of producing hydrogen [1–4,6]; this is primarily due to using water as an inexhaustible starting material instead of fossil fuels, and due to the integration of other renewable energy sources such as wind, solar, or tidal energy to facilitate the water-splitting

reaction. This is true since, in water electrolysis, hydrogen is generally produced by splitting water molecules into two components, i.e., hydrogen and oxygen gas, with the help of electricity [7]. Nevertheless, the current main challenges of applying such technology for large-scale industrial hydrogen production are primarily the high energy requirements that drive the electrochemical reaction for water splitting [3,4,7,8].

Typically, electrocatalysts are employed to overcome the high energy requirement for the hydrogen evolution reaction in electrochemical water splitting. Among the different types of electrocatalysts, noble metal-based electrocatalysts such as platinum and palladium have been widely considered one of the most active catalytic materials in both the hydrogen evolution reaction (HER) and the oxygen evolution reaction (OER) during water electrolysis [2,9,10]. However, such materials are often considered to be uneconomical for large-scale applications due to their scarcity and expense. Therefore, tremendous efforts have been carried out during the past several years to explore new and inexpensive alternative catalytic materials with similar or better activity than noble metal-based materials for the HER. Recently, other materials such as earth-abundant transition metals and metal oxides, carbon-based materials such as graphite or graphene oxide, and several types of organometallic compounds with specific characteristics have been successfully explored as potential candidates to substitute noble metal-based electrocatalysts [11–13].

Earth-abundant metal oxide-based materials have recently attracted much attention due to their inexpensiveness, long-term durability, high tolerance and stability against high applied potentials, and environmental friendliness. For example, spinel nickel ferrite oxide (NiFe_2O_4) has received significant attention as an emerging electrocatalyst material for the HER—especially in alkaline conditions [14–17]. In a previous report, sulfidized NiFe_2O_4 showed good catalytic activity in the HER, with an overpotential at 10 mA/cm² of 250 mV [16]. In another study, compositing NiFe_2O_4 and carbon black demonstrated reasonable physical-stability control for inhibiting the agglomeration process, which ultimately led to excellent HER catalytic activity compared to bare carbon black materials [5]. However, most of those metal oxide-based electrocatalysts still have far from the desired overpotential for economical hydrogen production. Recently, studies have shown that the catalytic activity of metal oxide-based electrocatalysts could be improved by increasing their active surface area through the introduction of mesoporosity feature [18–21]. This can easily be achieved by synthesizing the oxide via the nanocasting technique, using mesoporous silica as a hard template [18,19]. For instance, Kamali, H et al. reported that NiFe_2O_4 with mesoporous features provides a high surface active area, excellent conductivity, and good stability in its electrocatalytic performance [18].

In addition, studies have reported that compositing various types of electrocatalytic materials with carbon-based materials, such as graphene oxides, could be used as one strategy for further improving their HER activity [6,22,23]. For example, Du, Zuokai et al. investigated the combination of bimetallic metals with reduced graphene oxide materials for the electrocatalytic hydrogen reaction [15]. Based on their study, the catalyst was able to expose a promising result, with a considerably high overpotential of -112 mV vs. RHE. In other reports, Franceschini and co-workers modified GO with nickel warts to achieve a better electrocatalytic performance in stirring reactors, with an overpotential at 10 mA of -0.55 V vs. RHE [2].

In this study, graphene oxide was synthesized via Hummer's Methods in acidic conditions. The GO was combined with nickel ferrite oxide materials into composites to generate good performance in the hydrogen evolution reaction. Furthermore, the particle size of NiFe_2O_4 can be controlled to make it a mesoporous material by using hard template silica, which maintains the homogeneous particle size that is affected by the lower probability of aggregation [18,20]. This modification complements GO as a stabilizer material in the catalytic reaction and shows good conductivity due the presence of sp² carbon bonding and a deflection lattice structure [12,23]. As such, this procedure makes it possible to give information on the effects of homogenous mesoporous materials with a high active surface area on the performance of H₂O reduction to hydrogen species.

2. Materials and Methods

2.1. Chemicals and Reagents

In this study, nanoparticles were synthesized from $\text{Ni}(\text{NO}_3)_2 \cdot 10\text{H}_2\text{O}$, $\text{Fe}(\text{NO}_3)_3 \cdot 9\text{H}_2\text{O}$, ethanol, NaOH, NaNO_3 , H_2SO_4 , H_2O_2 , KMnO_4 , and HCl purchased from Merck (Rahway, NJ, USA). Graphite flakes were purchased from Sigma-Aldrich (St. Louis, MO, USA), DI water was purified with a Merck Millipore, electrode fabrication was performed using alumina powder (Saint-Gobain, Courbevoie, France), and Nafion was purchased from Huaian Kerun Membrane Material Co., Ltd. (Huai'an, China).

2.2. Synthesis of Mesoporous NiFe_2O_4

Mesoporous NiFe_2O_4 was synthesized using a hard template SBA 15 by the impregnation process; in the first step, the silica template was impregnated using a mixture containing 0.2 g $\text{Ni}(\text{NO}_3)_2 \cdot 10\text{H}_2\text{O}$ and 0.55 g $\text{Fe}(\text{NO}_3)_3 \cdot 9\text{H}_2\text{O}$ dissolved into 5 mL of ethanol. Then, 0.5 g of SBA-15 was added and stirred for 12 h and then dried overnight at 60 °C; after this, the product was calcined at 250 °C at a heating rate of 1 °C/min. The next step was the reimpregnation of the first impregnation product, with a similar impregnation step as before. The final powder product was calcined at 600 °C with a heating rate of 1 °C/min. The last step was the fabrication of the mesoporous NiFe_2O_4 : the hard template was etched away in a 2 M NaOH solution at 40 °C and stirred for 24 h, and in the final step, the powder product was washed with H_2O before continuing with a drying treatment overnight at room temperature [6].

2.3. Synthesis of Graphene Oxide

Hummer's method was performed to synthesize the graphene oxide (GO), followed by the oxidation and exfoliation of the graphite [24,25]. Firstly, 5 g of graphite was mixed with 2.5 g NaNO_3 into a 1 L beaker in an ice bath chamber. The mixture was stirred for 1 h after the addition of 0.2 L H_2SO_4 . This step was followed with the combination of a slow addition of 30 g of KMnO_4 and stirring for 2 h at 15 °C. After this, the mixture was continually stirred for 20 h at room temperature. Then, the system was heated to 70 °C and stirred for 2 h, followed by the slow addition of 100 mL H_2O . The heating process was applied to the mixture at 90 °C for 1 h with the slow addition of 100 mL H_2O ; both processes were performed using a stirring procedure. In the final process, 30 mL of H_2O_2 was added to finish the reaction. To obtain the GO powder, the mixture was repeatedly washed by centrifugation using HCl and the mixture was neutralized using H_2O ; this step was repeated several times until the mixture reached pH 7 and formed a gel compound, then the gel was dried for 24 h at 60 °C.

Graphene oxide decoration was carried out using ultrasonication between the GO and NiFe_2O_4 , at a 1:1 (*m/m*) ratio in 50 mL of ethanol for 1 h, to form a precipitate. Then, the precipitate was centrifuged at 6000 rpm. Then, the mixture was washed several times using ethanol and dried in an oven at 60 °C.

2.4. Electrode Fabrication GCE with the GO-Decorated NiFe_2O_4

The glassy carbon electrode (GCE) was prepared by being polished with alumina powder and then cleaned up using deionized water and ethanol using ultrasonication, respectively. Then, 5 mg of each previously prepared electrocatalyst material (GO, NiFe_2O_4 mesoporous, and GO/ NiFe_2O_4 composite) was added to 1 mL of H_2O . Next, the prepared glassy carbon electrode surface was dripped into the electrocatalyst colloid. Then, each electrode was dripped into 10 μL Nafion and dried at room temperature to produce three different electrodes called GCE/GO, GCE/ NiFe_2O_4 , and GCE/GO/ NiFe_2O_4 .

2.5. Characterization

The determination of the effects of specific lattice factors on the fabricated materials was studied using an X-ray diffractometer (XRD) PANalytical XPERT PRO. The characteristic bands and functional groups contained in each composite were studied using Raman

spectroscopy HORIBA The Lab HR Evolution Raman Microscopes and an FTIR Shimadzu IR Prestige 21, while the surface characterization of the GO decorated using mesoporous materials was conducted using a TEM Tecnai G2 SuperTwin and a BET Quantacrome Quadrasorb Evo, respectively.

2.6. Electrochemical Measurements

Electrochemical behavior was investigated using a three-electrode electrochemical system using a Potentiostat PGSTAT 204 Autolab and PalmSense 4, where Pt wire and an Ag/AgCl electrode were used as the counter and reference electrodes, respectively. Previously prepared GCE electrodes with a 0.5 cm physical diameter and 0.1964 cm² surface area were modified using synthesized materials such as GO, NiFe₂O₄, and GO/NiFe₂O₄, which were applied as working electrodes. The hydrogen evolution process was evaluated using 1 M NaOH solution as an electrolyte. Linear sweep voltammetry (LSV) and cyclic voltammetry (CV) were performed at a potential range of +0.5 V to (−0.8) V vs. RHE to explore the electrochemical characteristics of the modified electrode. Furthermore, the performance of the proposed electrode was investigated using the chronoamperometric technique (CA) for 9000 s. Electrochemical impedance spectroscopy testing was applied to determine the conductivity and the reactions that contributed to the HER reaction performance of each electrode.

3. Results and Discussion

3.1. Characterization of Mesoporous GO/NiFe₂O₄

The mesoporous NiFe₂O₄ starting material was successfully synthesized using SBA 15 as a hard template; it can be shown that there was no specific peak less than 30° on the diffractogram (Figure 1a) [21]. For the NiFe₂O₄, where the diffraction pattern could be found at 30.3° (220), 35.8° (331), 37.35° (222), 43.4° (400), 53.8° (442), 57.6° (511), and 63.1° (440)—linear to the crystal planes of the spinel NiFe₂O₄—this result was in line with the standard (Ref Code: 44-1485) and JCPDS 010-0325 [26,27]. The graphene oxide was clearly formed, as confirmed by the specific fingerprint peaks around 18° and 24.5°, referring to the lattice factors (011) and (002); the blunt peak (002) revealed at 24.5° indicated that the interaction between the carbon layer and the oxygen functional group was not fully integrated to form graphene oxide [28]. Hence, a shifting peak from 26.5° to 18° was observed due to the preformed random structure of the graphene being ordered into a folding graphene oxide layer sheet [28]. This attribute was caused by the formation of graphene oxide, which requires further optimization to drive the exfoliation of the carbon planar layer. Thus, if both of these processes are inhibited by the precursor, it will shift the lattice factor of the XRD pattern to 2θ-higher than the usual GO peak pattern [11,13]. The proposed material consisted of both of the fingerprint areas of the starting material (Figure 1a), so it can be concluded that the GO was successfully decorated with the mesoporous NiFe₂O₄.

The Raman spectra of the mesoporous GO/NiFe₂O₄ was divided into five specific bands consisting of A_{1g}, E_g, (3)F_{2g}, (2)F_{2g}, and (1)F_{2g} at the Raman shifts 240, 370, 475, 563, and 685 cm^{−1}, respectively (Figure 1b) [26,27]. Symmetric stretching of the oxygen atom along the tetrahedral Fe-O, linear to the A_{1g} band, occurred; meanwhile, an E_g and F_{2g} (3) band arose due to the symmetric and asymmetric bending of the oxygen. The F_{2g} (2) band occurred due to the asymmetric stretching of the Fe-O bond, and the last F_{2g} (1) band refers to the distribution of translational rotation molecules along the entire tetrahedron at the symmetrical structure on the material. Additionally, the specific Raman shifts of graphene oxide, called the D and G bands, were observed at 1345 cm^{−1} and 1602 cm^{−1}, respectively. Meanwhile, the D band showed a correlation with lattice defects in carbon and the sp² orbital contributor of the G band, producing an I_D/I_G ratio of 0.95—suggesting the formation of GO. These Raman spectra declared and confirmed by XRD characterization that the GO material was successfully fabricated using Hummer's method, as shown by

the existence of a 2D band on the GO Raman spectra [29]; this band only can be found on the graphene oxide material.

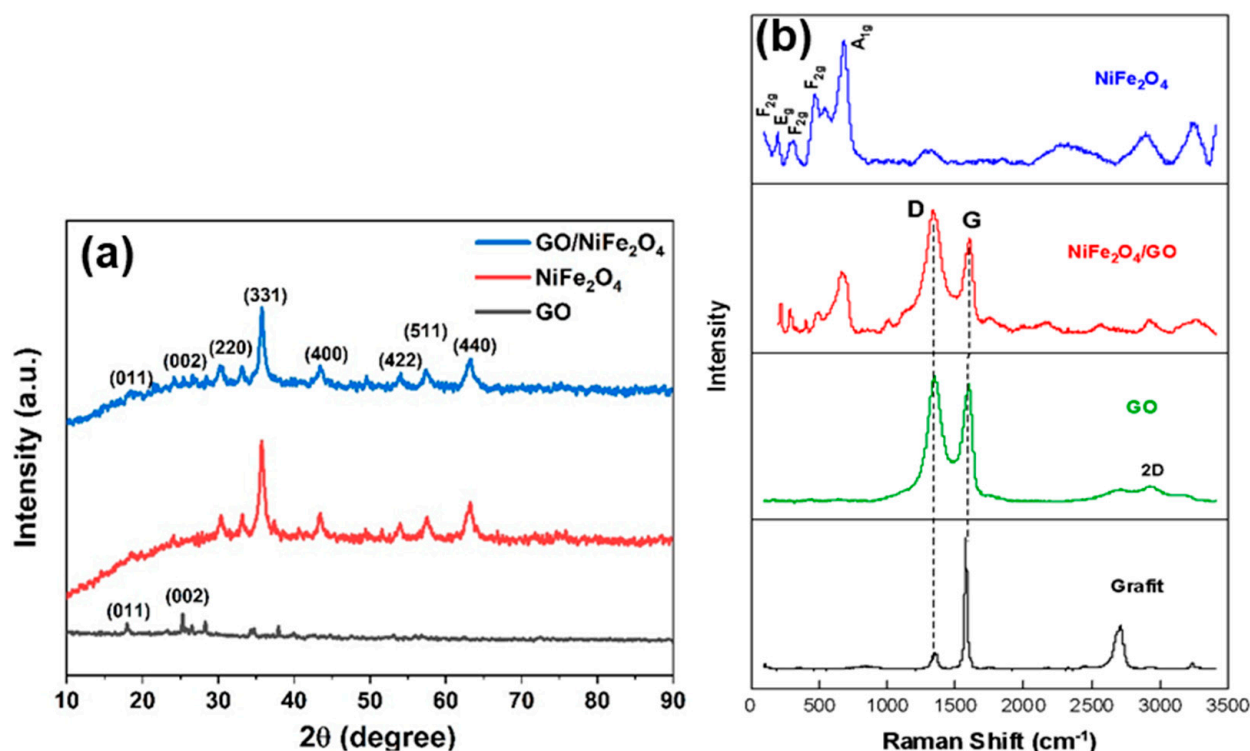


Figure 1. (a) XRD pattern (b) Raman Spectroscopy of mesoporous NiFe₂O₄/GO compared to their starting materials.

Figure 2a shows the FTIR spectra of the synthesized materials. In graphene oxide, there are several peaks indicating the presence of functional groups. At a wave number of 1030 cm⁻¹ and 1725 cm⁻¹, there was an absorption peak of stretched C=O and C-O bonds from the carbonyl molecules, which indicates the presence of oxygen functional groups after oxidation; this means that the intercalation of oxygen molecules occurred on the carbon layer [29]. At a wave number of 1625 cm⁻¹, there was an absorption peak for C=C, which indicates that it remained C=C both before and after oxidation. Meanwhile, at wave number 3364 cm⁻¹, there was an O-H absorption peak in the presence of a carboxyl group on the graphene oxide, caused by the oxidation process that occurred during the synthesis of the graphene oxide. For the GO/NiFe₂O₄ composites, there was an absorption peak at the wave number of 587 cm⁻¹, which indicates that the functional group Fe-O came from the NiFe₂O₄ nanoparticles. At a wave number of 1609 cm⁻¹, the absorption peak of C=C came from the graphene oxide. Then, at wave number 3202 cm⁻¹, there was an O-H absorption peak that came from the carboxyl group on the graphene oxide.

In the FTIR results for the GO/NiFe₂O₄, the O-H and C=O peaks were shifting and reduced, which means that the GO was decorated by the NiFe₂O₄. The porous characteristics of the NiFe₂O₄ and GO/NiFe₂O₄ were confirmed using the adsorption-desorption isotherm of N₂, subsequently displaying a type-IV isotherm (IUPAC classification; Figure 2b) with the presence of mesoporous characteristics and a specific surface area calculated from BET measurements [18,19]. As seen in Table 1, the surface areas of the graphene oxide, NiFe₂O₄, and GO/NiFe₂O₄ were 0.0406, 55.830, and 38.729 m²/g, respectively. Mesoporous NiFe₂O₄ without GO had a higher surface area than the GO/NiFe₂O₄ composites; this was caused by the GO interlayer structure being altered by the NiFe₂O₄ mesoporous structure that was synthesized using the SBA-15 template.

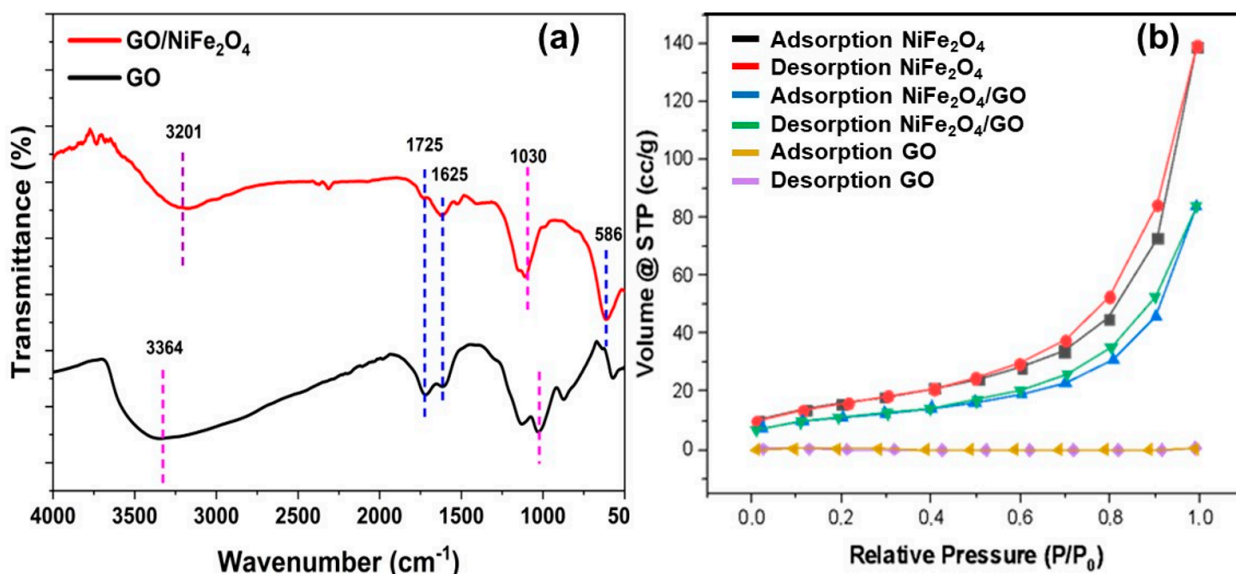


Figure 2. (a) FTIR (b) BET of the mesoporous GO/NiFe₂O₄ compared to their starting materials.

Table 1. Measurement of the surface area of the materials.

Materials	Surface Area (m ² /g)
GO	0.0406
mesoporous NiFe ₂ O ₄	55.830
GO/mesoporous NiFe ₂ O ₄	38.729

The graphene oxide that was synthesized consisted of a layer sheet structure, imaged in Figure 3a; this structure serves to enhance the surface active area where the reaction began. Besides the structure of NiFe₂O₄ being specifically like a tube (Figure 3b)—similar to the SBA-15 template with the 5 nm diameter—based on the calculation of particle size using Image-J software (Figure 3b), this material formed with a major particle size of less than 5 nm—showing that the NiFe₂O₄ was successfully synthesized using hard template SBA-15. The graphene oxide layer was decorated using a mixing procedure with the mesoporous NiFe₂O₄; thus, the layer spacing on the GO was increased by the addition of NiFe₂O₄ particles—improving the pore size of the modified electrode, which can be seen in Figure 2b and Table 1, where the adsorption and desorption of the GO increased after being modified with NiFe₂O₄.

The oxidation reaction of the graphite was followed by an exfoliation process, forming graphene oxide; each procedure was applied to allow the addition of oxygen atoms into the graphene layer structure after initiation, using an exfoliation process in acidic conditions. This treatment was completed with the addition of NiFe₂O₄ to the mesoporous structure, in order to re-enlarge the d-spacing between the graphene oxide surface layers. The presence of oxygen atoms in the graphene oxide was the main method for enhancing the electron transfer of the material, followed by the existence of three lone pairs of electrons on the oxygen atoms. When the intercalation of the oxygen atom was completed by the mesoporous NiFe₂O₄, the active surface area and the transfer of electrons on the decorated graphene oxide material was enhanced as a result of the presence of the NiFe₂O₄ crystal structure on their interlayer surface.

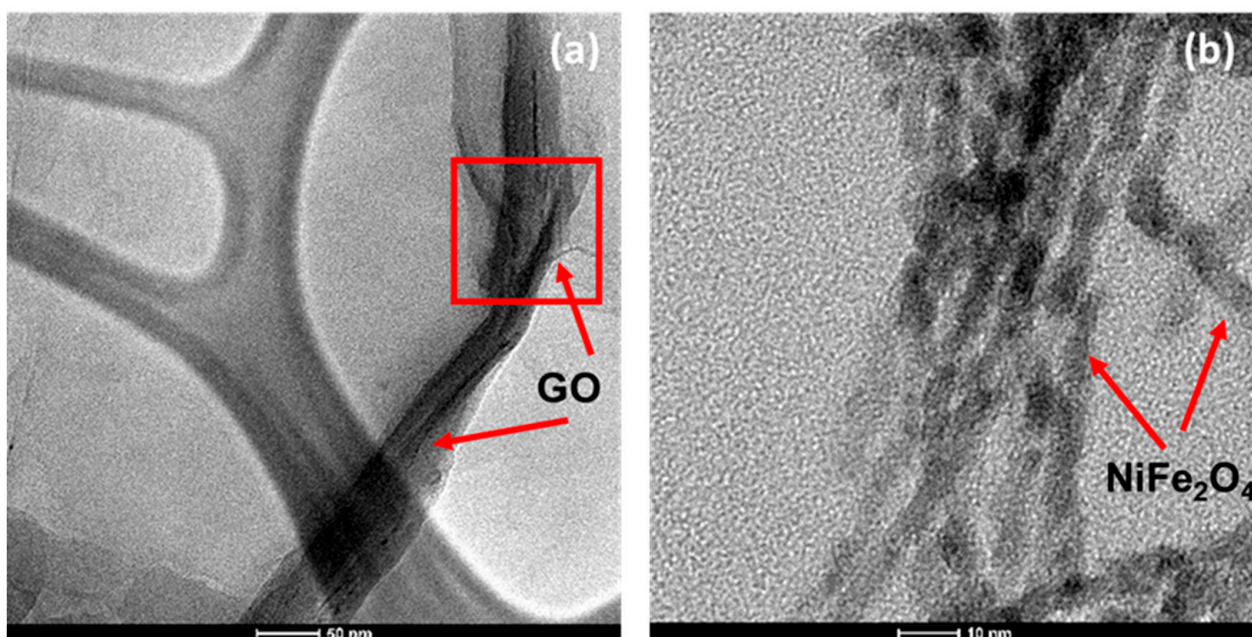


Figure 3. TEM image of (a) Graphene Oxide and (b) NiFe₂O₄.

3.2. The Electrochemical Performance of GO/NiFe₂O₄ in the Hydrogen Evolution Reaction

The electrocatalytic HER activity at various electrodes was investigated using a three-electrode electrochemical system in 1 M NaOH solution. The LSV technique was applied to determine the performance of the various electrodes in the HER reaction at a potential range from +0.5V to (−0.8) V vs. RHE. Figure 4a shows that GCE/GO/NiFe₂O₄ had the most positive onset potential compared to the other electrodes, at −0.020 V, while the bare GCE, GCE/GO, and GCE/NiFe₂O₄ had a potential of −0.296 V, −0.331 V, and −0.087 V, respectively. This indicates that the modified glassy carbon electrode with the GO/NiFe₂O₄ composite showed better performance with a lower onset potential, which means that the modified electrode needed less of an energy potential to produce hydrogen gas.

The influence of particle size/surface area is correlated to the electrochemically active surface area, which can interfere with the electrocatalytic performance. With a controlled material size, we can reduce the probability of the agglomeration process occurring on the supporting material. This agglomeration would inhibit the redox reaction on the surface of the modified electrode, increasing the energy that we need to produce hydrogen through the HER reaction. The increase in the energy required is linear to how much current can be transferred from the electrode to the electrolyte system to start the hydrogen evolution reaction. In conclusion, the highest electrochemical active surface area will be linear to the lowest overpotential value.

The chronoamperometric technique was performed to see how stable an electrode can be when producing hydrogen gas in the HER reaction. Based on Figure 4c, the GCE/GO/NiFe₂O₄ provided greater stability for 9000 s. The stability of the proposed electrode was caused by the contribution of the GO material, as carbon-based materials that consist of sp² carbon binding can deliver more electrons to the electrolyte [30]. Even though GO performs well in the electrochemical reaction, the carbon derivate needs to be electrochemically preconditioned further before being used in the hydrogen evolution reaction; thus, a higher current in the early stability test is appropriate with higher preconditioning times, so the electrode can get ready to stabilize the reduction reaction—as can be seen by the current drop that occurred on the chronoamperogram in Figure 4c. In fact, the graphene oxide layer was dispersed by the mesoporous NiFe₂O₄, as the impact of the decoration process produced a more active site that contributed to the stabilization of the hydrogen evolution reaction.

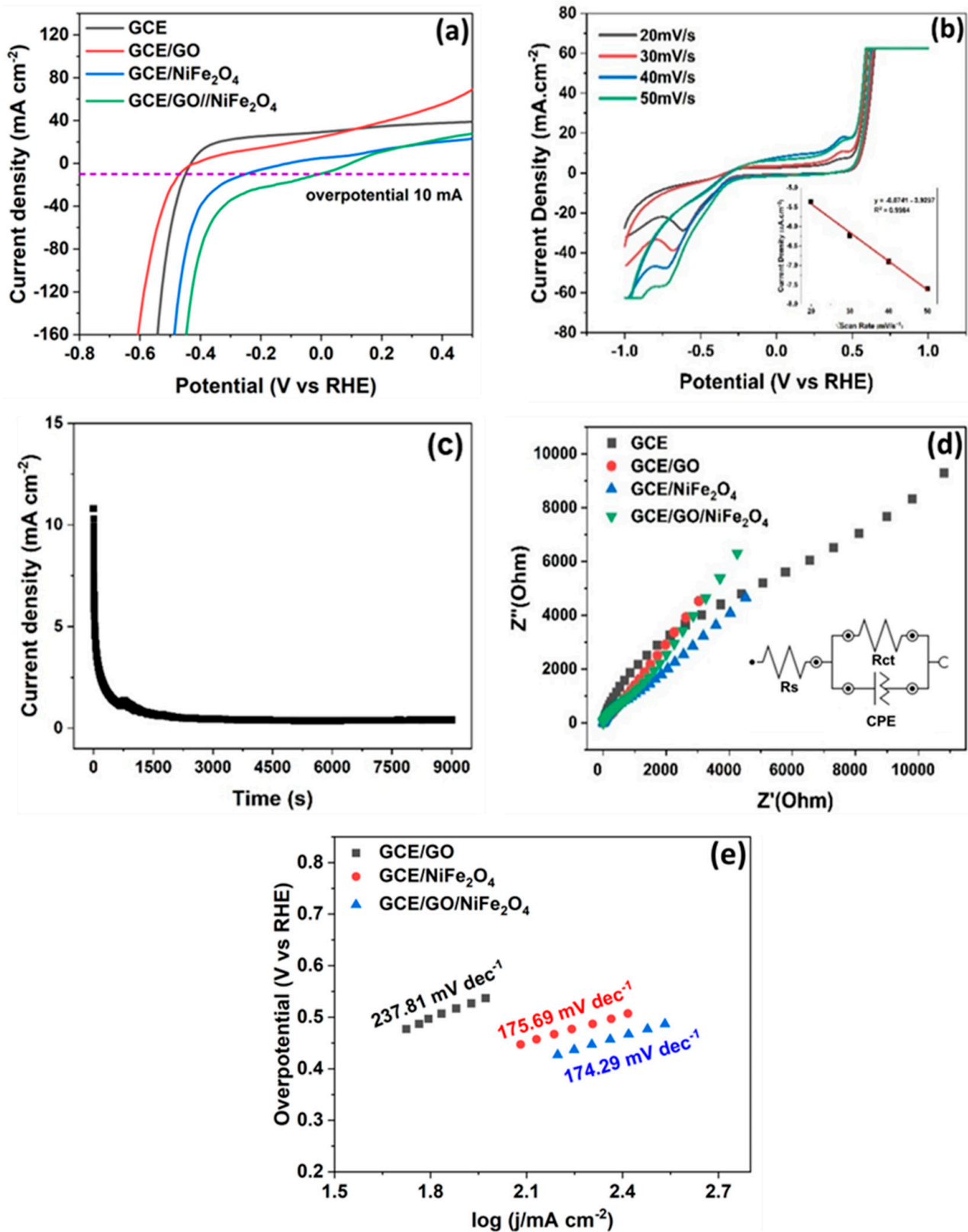


Figure 4. Electrochemical behavior of $\text{NiFe}_2\text{O}_4/\text{GO}$ in 1M NaOH (a) LSV curve (b) Cyclic Voltammogram, (c) Stability test using chronoamperometry for 9000 s (d) Nyquist plot, and (e) Tafel plot.

The Nyquist plot of the electrode variation is the result of the application of a frequency range of 100 kHz to 0.1 Hz to each working electrode. The modified glassy carbon electrode with the GO/NiFe₂O₄ composite showed better impedance characteristics than the other working electrodes. The Figure 4d inset reveals the fitting circuit, which consists of three different resistance systems such as the R_s (solution resistance), R_{ct} (charge transfer resistance), and CPE (constant phase element resistance) [31]. These circuits are exhibited in the Nyquist plot extrapolation in Figure 4d, which depicts one semicircular line for the high frequency data and a straight line for the lower frequency data. The high frequency of the EIS technique informs the surface reaction, which generates the charge transfer reaction; furthermore, the low frequency dictates the diffusion mechanism [31]. It can be shown in Figure 4d that we can find a semicircular pattern for the high frequency electrode that is more upright than that of another electrode at a lower frequency, which means that the kinetic electron transfer was a combination of the redox reaction from the NiFe₂O₄ and a diffusion mechanism at the electrical double layer of the graphene oxide [31].

The cyclic voltammetry method was carried out to see the ratio of the peak currents at various scan rates; linear extrapolation was used to calculate the electrochemical active surface area (ECSA) of the electrode (Figure 4b), following the Randles–Sevcik equation below:

$$i_p = 2.687 \times 10^5 n^{\frac{3}{2}} A D^{\frac{1}{2}} C v^{\frac{1}{2}}$$

where i_p is the peak current, n is the number of transferred electrons coefficient ($6.5 \times 10^{-6} \text{ cm}^2 \cdot \text{s}^{-1}$), C is the concentration of the redox solution, and v is the scan rate [32]. The ECSA defined the population of the active site in the structure of the proposed electrode, which was able to retain the electrochemical reaction. Table 2 shows that the GCE/GO/NiFe₂O₄ had the highest electroactive surface area compared to the other electrodes; this result was linear with respect to the decoration of the Graphene Oxide structure using NiFe₂O₄. The decoration process resulted in the enhancement of the GO surface, providing a more active site (Figure 4b); this was demonstrated by the active surface area of the GCE/GO/NiFe₂O₄ being two times higher than the GCE/GO electrode.

Table 2. Comparison of the electrode electrochemically active surface area (ECSA).

Electrode	Linearity	ECSA (cm ²)
GCE	0.9984	1.89×10^{-4}
GCE/GO	0.9882	1.78×10^{-4}
GCE/NiFe ₂ O ₄	0.9838	2.24×10^{-4}
GCE/GO/NiFe ₂ O ₄	0.9964	3.18×10^{-4}

Besides this, the conductivity of the graphene oxide material was boosted by the NiFe₂O₄ material, resulting in the surface integration of the GO layer, supported by the NiFe₂O₄; this result was linear to the Tafel Extrapolation of the energy of the undecorated GO, at 237.81 mV dec⁻¹, which was strongly decreased to 174.29 mV dec⁻¹ after being altered by NiFe₂O₄—as seen in Figure 4e. Moreover, this increase in the catalytic performance of the GO/NiFe₂O₄ was conducted via the surface functionalization of the GO with nickel ferrite oxide; it seems this material shows good catalytic completion, as shown by its Tafel plot value of 175.69 mV dec⁻¹. The Tafel plot is used as a method to evaluate the ORR or HER reaction; it is calculated using the overpotential calculation, where the smallest overpotential indicates the best performance, as the materials need lower energy to begin both of the reactions [19].

The catalytic performance of the proposed material was favorable compared to that of other reported electrode catalysts. Table 3 shows that by using mesoporous materials, NiFe₂O₄ can enhance the performance of the hydrogen evolution reaction when combined with another catalyst electrode. The Tafel slope of the GO/NiFe₂O₄ was comparable to the NF base material, had a bigger Tafel slope value than the others, and still needed to be optimized to achieve better performance. The structure modification of the mesoporous

NiFe₂O₄ was carried out using simple hydrothermal methods, and the mesoporous size was controlled by hard template SBA-15. This procedure is very important, because the decoration of the GO layer using the NiFe₂O₄ substrate had a linear relationship with the improvement of electrocatalytic performance. First, the electrochemically active surface area was enhanced by two-fold more than the GO material without NiFe₂O₄ decoration. Those hydrogen evolution reaction performances will increase linearly to the population of the active sites on the electrode surface; this resulted in the HER performance of GO/NiFe₂O₄ being increased compared to the bare GO, which can be seen by the overpotential at 10 mA/cm² decreasing from −0.470 V to −0.036 V. In this last one, the presence of homogeneous NiFe₂O₄ on the mesoporous structure maintained the stability performance of the hydrogen evolution reaction. The effect of the intercalation process on the d spacing layer of the graphene oxide, followed by mixing it using homogeneous mesoporous particles, gives a good response to the electrocatalytic HER performance. This will allow other research works to use this report to enhance the catalytic performance, followed by the homogeneity control, of their supporting materials.

Table 3. Comparison performance of the hydrogen evolution reaction in the modified electrodes.

Electrode	Electrolyte	η_{10} (mV)	Tafel Slope (mV dec ^{−1})	Ref
NiFe ₂ O ₄ /NF	1 M KOH	379	139	[33]
NiFe ₂ O ₄ /CB	0.5 M H ₂ SO ₄	187	85.8	[5]
NiFe ₂ O ₄ /NiFe	1 M KOH	130	112.4	[33]
NCS/rGO	1 M NaOH	241	110	[34]
rGO(paper)	0.5 M H ₂ SO ₄	510	–	[35]
MoS ₂ NF/rGO paper	0.5 M H ₂ SO ₄	190	95	[35]
GO/NiFe ₂ O ₄	1 M NaOH	36	174.3	This work

4. Conclusions

Mesoporous NiFe₂O₄ was successfully synthesized through the nano-casting method and successfully fabricated with graphene oxide to form GO/NiFe₂O₄ composites. The good fabrication of NiFe₂O₄ and GO was shown using XRD and confirmed using FTIR and Raman spectroscopy. The high surface area, determined using BET measurements, was linear to calculations of the electrochemically active surface area—at 3.18×10^{-4} cm²—as determined by the Randles–Sevcik equation. The proposed catalyst showed good HER catalytic activity by generating an overpotential at 10 mA of −0.036 V for the GO/NiFe₂O₄, as compared to the other electrode. Regarding the charge transfer measurements, the decoration of the GO sheet with mesoporous NiFe₂O₄ produced specific electrochemical behaviors such as better ionic conductivity with lower resistance and a smaller leaching surface—determined based on the stable current that was recorded when the stability test was applied for 9000 s.

Author Contributions: Conceptualization, T.A.I., G.T.M.K., F.A., Y.A. and M.K.; methodology, G.T.M.K., U.P. and M.K.; formal analysis, all authors.; data acquisition, A.R.S. and S.A.; writing—review and editing, A.R.S. and S.A.; funding acquisition, G.T.M.K., U.P. and M.K. All authors have read and agreed to the published version of the manuscript.

Funding: The author would like to acknowledge the support of this work provided by the Directorate of Research and Development, Universitas Indonesia, under the Riset Kolaborasi Indonesia Program (RKI) 2022 (Contract No NKB—1067/UN2.RST/HKP.05.00/2022).

Data Availability Statement: The data is available upon request.

Conflicts of Interest: The authors declare no conflict of interest.

References

1. Huang, H.; Yan, M.; Yang, C.; He, H.; Jiang, Q.; Yang, L.; Lu, Z.; Sun, Z.; Xu, X.; Bando, Y.; et al. Graphene Nanoarchitectonics: Recent Advances in Graphene-Based Electrocatalysts for Hydrogen Evolution Reaction. *Adv. Mater.* **2019**, *31*, 1903415. [[CrossRef](#)]
2. Franceschini, E.A.; Lacconi, G.I. Synthesis and Performance of Nickel/Reduced Graphene Oxide Hybrid for Hydrogen Evolution Reaction. *Electrocatalysis* **2018**, *9*, 47–58. [[CrossRef](#)]
3. Jang, D.; Kim, K.; Kim, K.H.; Kang, S. Techno-Economic Analysis and Monte Carlo Simulation for Green Hydrogen Production Using Offshore Wind Power Plant. *Energy Convers. Manag.* **2022**, *263*, 115695. [[CrossRef](#)]
4. Vazini Modabber, H.; Alireza Mousavi Rabeti, S. New Optimal Scheme for the Poly-Generation System, Integrated with ORC and Hydrogen Production Units, Using Technical, Energy, and Thermo-Risk Analyses-Case Study for Qeshm Power and Water Co-Generation Plant. *Therm. Sci. Eng. Prog.* **2022**, *36*, 101506. [[CrossRef](#)]
5. Munonde, T.S.; Zheng, H.; Matseke, M.S.; Nomngongo, P.N.; Wang, Y.; Tsiakaras, P. A Green Approach for Enhancing the Electrocatalytic Activity and Stability of NiFe₂O₄/CB Nanospheres towards Hydrogen Production. *Renew. Energy* **2020**, *154*, 704–714. [[CrossRef](#)]
6. Flis-Kabulska, I.; Gajek, A.; Flis, J. Understanding the Enhancement of Electrocatalytic Activity toward Hydrogen Evolution in Alkaline Water Splitting by Anodically Formed Oxides on Ni and C-Containing Ni. *ChemElectroChem* **2021**, *8*, 3371–3378. [[CrossRef](#)]
7. Kuleshova, T.E.; Ivanova, A.G.; Galushko, A.S.; Kruchinina, I.Y.; Shilova, O.A.; Udalova, O.R.; Zhestkov, A.S.; Panova, G.G.; Gall, N.R. Influence of the Electrode Systems Parameters on the Electricity Generation and the Possibility of Hydrogen Production in a Plant-Microbial Fuel Cell. *Int. J. Hydrogen Energy* **2022**, *47*, 24297–24309. [[CrossRef](#)]
8. Demir, M.E.; Dincer, I. An Integrated Solar Energy, Wastewater Treatment and Desalination Plant for Hydrogen and Freshwater Production. *Energy Convers. Manag.* **2022**, *267*, 115894. [[CrossRef](#)]
9. Elbert, K.; Hu, J.; Ma, Z.; Zhang, Y.; Chen, G.; An, W.; Liu, P.; Isaacs, H.S.; Adzic, R.R.; Wang, J.X. Elucidating Hydrogen Oxidation/Evolution Kinetics in Base and Acid by Enhanced Activities at the Optimized Pt Shell Thickness on the Ru Core. *ACS Catal.* **2015**, *5*, 6764–6772. [[CrossRef](#)]
10. Deng, B.L.; Guo, L.P.; Lu, Y.; Rong, H.B.; Cheng, D.C. Sulfur–Nitrogen Co-Doped Graphene Supported Cobalt–Nickel Sulfide RGO@SN-CoNi₂S₄ as Highly Efficient Bifunctional Catalysts for Hydrogen/Oxygen Evolution Reactions. *Rare Met.* **2022**, *41*, 911–920. [[CrossRef](#)]
11. Gao, X.; Jang, J.; Nagase, S. Hydrazine and Thermal Reduction of Graphene Oxide: Reaction Mechanisms, Product Structures, and Reaction Design. *J. Phys. Chem. C* **2010**, *114*, 832–842. [[CrossRef](#)]
12. Khani, H.; Grundish, N.S.; Wipf, D.O.; Goodenough, J.B. Graphitic-Shell Encapsulation of Metal Electrocatalysts for Oxygen Evolution, Oxygen Reduction, and Hydrogen Evolution in Alkaline Solution. *Adv. Energy Mater.* **2020**, *10*, 1903215. [[CrossRef](#)]
13. Hsiao, M.C.; Liao, S.H.; Yen, M.Y.; Liu, P.I.; Pu, N.W.; Wang, C.A.; Ma, C.C.M. Preparation of Covalently Functionalized Graphene Using Residual Oxygen-Containing Functional Groups. *ACS Appl. Mater. Interfaces* **2010**, *2*, 3092–3099. [[CrossRef](#)] [[PubMed](#)]
14. Khazenipour, K.; Moeinpour, F.; Mohseni-Shahri, F.S. Cu(II)-Supported Graphene Quantum Dots Modified NiFe₂O₄: A Green and Efficient Catalyst for the Synthesis of 4H-Pyrimido[2,1-b]Benzothiazoles in Water. *J. Chin. Chem. Soc.* **2021**, *68*, 121–130. [[CrossRef](#)]
15. Du, Z.; Wang, Y.; Li, J.; Liu, J. Facile Fabrication of Pt–Ni Alloy Nanoparticles Supported on Reduced Graphene Oxide as Excellent Electrocatalysts for Hydrogen Evolution Reaction in Alkaline Environment. *J. Nanoparticle Res.* **2019**, *21*, 13. [[CrossRef](#)]
16. Tetzlaff, D.; Alagarasan, V.; Simon, C.; Siegmund, D.; Puring, K.J.; Marschall, R.; Apfel, U.P. [NiFe]-(Oxy)Sulfides Derived from NiFe₂O₄ for the Alkaline Hydrogen Evolution Reaction. *Energies* **2022**, *15*, 543. [[CrossRef](#)]
17. Liu, B.; Peng, H.Q.; Cheng, J.; Zhang, K.; Chen, D.; Shen, D.; Wu, S.; Jiao, T.; Kong, X.; Gao, Q.; et al. Nitrogen-Doped Graphene-Encapsulated Nickel–Copper Alloy Nanoflower for Highly Efficient Electrochemical Hydrogen Evolution Reaction. *Small* **2019**, *15*, 1901545. [[CrossRef](#)] [[PubMed](#)]
18. Kamali-Heidari, E.; Kamyabi-Gol, A. Synthesis of Mesoporous Nickel Iron Oxide as a New Anode Material for High Performance Lithium Ion Batteries. *Phys. B Condens. Matter* **2019**, *570*, 176–181. [[CrossRef](#)]
19. Fadhli, Erika, D.; Mardiana, S.; Rasrendra, C.B.; Khalil, M.; Kadja, G.T.M. Nanocasting Nanoporous Nickel Oxides from Mesoporous Silicas and Their Comparative Catalytic Applications for the Reduction of P-Nitrophenol. *Chem. Phys. Lett.* **2022**, *803*, 139809. [[CrossRef](#)]
20. Shcherban, N.D.; Shvalagin, V.V.; Korzhak, G.V.; Yaremov, P.S.; Skoryk, M.A.; Sergiienko, S.A.; Ya. Kuchmiy, S. Hard Template Synthesis and Photocatalytic Activity of Graphitic Carbon Nitride in the Hydrogen Evolution Reaction Using Organic Acids as Electron Donors. *J. Mol. Struct.* **2022**, *1250*, 131741. [[CrossRef](#)]
21. Vélez-Peña, E.; Morales, R.; Reyes-Escobar, C.; Torres, C.C.; Avello, M.; Marrugo, K.P.; Manzo-Merino, J.; Alderete, J.B.; Campos, C.H. Mesoporous Mixed Oxides Prepared by Hard Template Methodology as Novel Drug Delivery Carriers for Methotrexate. *J. Drug Deliv. Sci. Technol.* **2022**, *73*, 103483. [[CrossRef](#)]
22. Singh, A.P.; Balayan, S.; Hooda, V.; Sarin, R.K.; Chauhan, N. Nano-Interface Driven Electrochemical Sensor for Pesticides Detection Based on the Acetylcholinesterase Enzyme Inhibition. *Int. J. Biol. Macromol.* **2020**, *164*, 3943–3952. [[CrossRef](#)]
23. Chen, H.; Shen, X.; Xu, K.; Chen, Y.; Yuan, A.; Ji, Z.; Wang, Z.; Zhu, G. NiFe–NiFe₂O₄/RGO Composites: Controlled Preparation and Superior Lithium Storage Properties. *J. Am. Ceram. Soc.* **2021**, *104*, 6696–6708. [[CrossRef](#)]

24. Zhang, Q.; Yang, Y.; Fan, H.; Feng, L.; Wen, G.; Qin, L.C. Synthesis of Graphene Oxide Using Boric Acid in Hummers Method. *Colloids Surf. A Physicochem. Eng. Asp.* **2022**, *652*, 129802. [[CrossRef](#)]
25. Zhu, Y.; Kong, G.; Pan, Y.; Liu, L.; Yang, B.; Zhang, S.; Lai, D.; Che, C. An Improved Hummers Method to Synthesize Graphene Oxide Using Much Less Concentrated Sulfuric Acid. *Chin. Chem. Lett.* **2022**, *33*, 4541–4544. [[CrossRef](#)]
26. Habibi, M.H.; Fakhri, F. Hydrothermal Synthesis of Nickel Iron Oxide Nano-Composite and Application as Magnetically Separable Photocatalyst for Degradation of Solar Blue G Dye. *J. Mater. Sci. Mater. Electron.* **2017**, *28*, 14091–14096. [[CrossRef](#)]
27. Sharma, P.; Minakshi Sundaram, M.; Watcharatharapong, T.; Laird, D.; Euchner, H.; Ahuja, R. Zn Metal Atom Doping on the Surface Plane of One-Dimensional NiMoO₄ Nanorods with Improved Redox Chemistry. *ACS Appl. Mater. Interfaces* **2020**, *12*, 44815–44829. [[CrossRef](#)]
28. Siburian, R.; Sihotang, H.; Lumban Raja, S.; Supeno, M.; Simanjuntak, C. New Route to Synthesize of Graphene Nano Sheets. *Orient. J. Chem.* **2018**, *34*, 182–187. [[CrossRef](#)]
29. Ahlawat, A.; Sathe, V.G. Raman Study of NiFe₂O₄ Nanoparticles, Bulk and Films: Effect of Laser Power. *J. Raman Spectrosc.* **2011**, *42*, 1087–1094. [[CrossRef](#)]
30. Sookhajian, M.; Mat Teridi, M.A.; Tong, G.B.; Woi, P.M.; Khalil, M.; Alias, Y. Reduced Graphene Oxide/Copper Nanoparticle Composites as Electrochemical Sensor Materials for Nitrate Detection. *ACS Appl. Nano Mater.* **2021**, *4*, 12737–12744. [[CrossRef](#)]
31. Bredar, A.R.C.; Chown, A.L.; Burton, A.R.; Farnum, B.H. Electrochemical Impedance Spectroscopy of Metal Oxide Electrodes for Energy Applications. *ACS Appl. Energy Mater.* **2020**, *3*, 66–98. [[CrossRef](#)]
32. Putri, Y.M.T.A.; Gunlazuardi, J.; Ivandini, T.A. Electrochemical Preparation of Highly Oriented Microporous Structure Nickel Oxide Films as Promising Electrodes in Urea Oxidation. *Chem. Lett.* **2022**, *51*, 135–138. [[CrossRef](#)]
33. Zhang, X.; Qiu, Y.; Li, Q.; Liu, F.; Ji, X.; Liu, J. Facile Construction of Well-Defined Hierarchical NiFe₂O₄/NiFe Layered Double Hydroxides with a Built-in Electric Field for Accelerating Water Splitting at the High Current Density. *Int. J. Hydrogen Energy* **2022**, *47*, 40826–40834. [[CrossRef](#)]
34. Shabnam, L.; Faisal, S.N.; Hoang, V.C.; Martucci, A.; Gomes, V.G. Doping Reduced Graphene Oxide and Graphitic Carbon Nitride Hybrid for Dual Functionality: High Performance Supercapacitance and Hydrogen Evolution Reaction. *J. Electroanal. Chem.* **2020**, *856*, 113503. [[CrossRef](#)]
35. Ma, C.B.; Qi, X.; Chen, B.; Bao, S.; Yin, Z.; Wu, X.J.; Luo, Z.; Wei, J.; Zhang, H.L.; Zhang, H. MoS₂ Nanoflower-Decorated Reduced Graphene Oxide Paper for High-Performance Hydrogen Evolution Reaction. *Nanoscale* **2014**, *6*, 5624–5629. [[CrossRef](#)] [[PubMed](#)]

Disclaimer/Publisher's Note: The statements, opinions and data contained in all publications are solely those of the individual author(s) and contributor(s) and not of MDPI and/or the editor(s). MDPI and/or the editor(s) disclaim responsibility for any injury to people or property resulting from any ideas, methods, instructions or products referred to in the content.